

Structural Analysis of von Willebrand Factor

Maria A. Brehm¹

¹Institute of Biology, School of Science and Technology, University of Siegen, Siegen, Germany

Hamostaseologie 2026;46:24–33.

Address for correspondence Maria A. Brehm, Institute of Biology, School of Science and Technology, University of Siegen, Artur-Woll-Haus, Raum AE-B 002, Am Eichenhang 50, 57076 Siegen, Germany (e-mail: maria.brehm@uni-siegen.de).

Abstract

The von Willebrand factor (VWF) is a large, multidomain glycoprotein whose modular organization facilitates its diverse physiological functions, primarily in hemostasis. Each domain contributes distinct molecular properties that collectively enable VWF to sense shear force, mediate platelet adhesion, and stabilize coagulation factor VIII (FVIII). In the past decades, structural studies using X-ray crystallography, cryo-electron microscopy (cryo-EM), nuclear magnetic resonance (NMR), and molecular modeling have revealed the architecture of nearly every domain. This review provides an examination of VWF's molecular architecture, the structural basis of its interactions, and the implications of structural insights for disease understanding and therapy.

Keywords

- ▶ domain structure
- ▶ VWF
- ▶ von Willebrand disease

Introduction

Hemostasis is a tightly regulated process that prevents excessive blood loss following vascular injury. A key player for the initiation of primary hemostasis is the von Willebrand factor (VWF), a multimeric glycoprotein produced exclusively by endothelial cells and megakaryocytes. The significance of VWF is highlighted by two extremes: (1) the bleeding disorder von Willebrand disease (VWD) resulting from absence or deficiency of VWF¹ and (2) the thrombotic microangiopathy thrombotic thrombocytopenic purpura (TTP) induced by VWF hyperactivity due to absence or dysfunction of ADAMTS13. The latter is a disintegrin and metalloprotease with thrombospondin type 1 motif 13 highly specific for VWF and responsible for regulating its multimer size in circulation.^{2–4} Its cleavage site on VWF lies within the A2 domain and becomes accessible only after A2 unfolds under high shear stress caused by the increased tensile force exerted on VWF when platelets bind.⁵

The challenge of studying VWF arises from its massive multimeric size, its complex post-translational modifications, and its mechanosensitive conformational states. Early biochemical characterizations laid the foundation for understanding VWF's role, but only with the advent of modern structural biology tools, like X-ray crystallography, cryo-electron microscopy (cryo-EM), nuclear magnetic resonance (NMR), and molecular simulations, it has been

possible to characterize its domains and their dynamic behavior.

This review synthesizes current knowledge of VWF structure and dynamics, emphasizing how structure governs function, how defects in structure cause disease, and how structural understanding guides modern therapy.

Molecular Architecture of VWF

VWF is synthesized as a pre-pro-polypeptide exclusively in endothelial cells (ECs) and megakaryocytes. Due to the latter, VWF is also found in platelets. The biosynthetic process includes the signal peptide, which directs the nascent chain into the endoplasmic reticulum (ER), the propeptide (D1–D2 assemblies), essential for multimerization and tubulation in Weibel-Palade bodies (WPBs), and the mature subunit, which is separated from the latter two due to cleavage by furin in the Golgi apparatus but stays non-covalently bound until release into the circulation. The mature subunit contains domains D'-D3-A1-A2-A3-D4-C1-C2-C3-C4-C5-C6-CK (▶ Fig. 1).⁶ Multimerization is central to VWF's function. Monomers are therefore first dimerized by protein disulfide isomerase isoform A1 (PDIA1) in the ER via disulfide bridges between the C-terminal CK domains.^{7,8} In the Golgi, dimers are then connected to multimers by N-terminal disulfide bonding, yielding multimers which can exceed sizes of 10,000 kD.⁹ These multimers are stored in WPBs within

received

November 2, 2025

accepted after revision

November 19, 2025

© 2026, Thieme. All rights reserved.

Georg Thieme Verlag KG,

Oswald-Hesse-Straße 50,

70469 Stuttgart, Germany

DOI <https://doi.org/10.1055/a-2751-7066>.

ISSN 0720-9355.

ISSN 0720-9355.

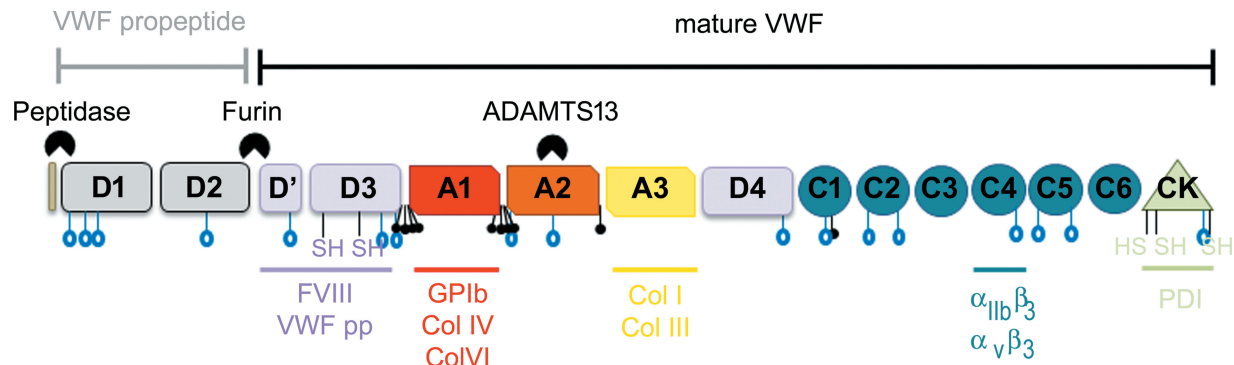


Fig. 1 Schematic presentation of the VWF domain structure. The VWF propeptide (VWF pp) is shown in gray, mature VWF is indicated by a black line. The black wedges mark cleavage sites for indicated proteases. N-glycosylation and O-glycosylation sites are indicated by blue and black lollipops, respectively. Cysteine residues essential for multimerization and dimerization are indicated by violet and green SH-groups in the D3 and CK domains, respectively. Ligands are indicated below the respective binding domains. ADAMTS13, a disintegrin and metalloprotease with thrombospondin type 1 motif 13; Col IV, VI, I, and III, collagens IV, VI, I and III; FVIII, coagulation factor VIII; GPIb, glycoprotein Ib; PDI, protein disulfide isomerase isoform A1; $\alpha_{IIb}\beta_3$, platelet integrin $\alpha_{IIb}\beta_3$; $\alpha_v\beta_3$, integrin $\alpha_v\beta_3$.

ECs or constitutively secreted.^{10,11} In platelets, VWF is stored in α -granules. Maturation of the multimers further involves posttranslational modifications such as sialylation, sulfation, and glycosylation. Complex glycans, linked to more than a dozen N-linked and multiple O-linked glycosylation sites, have been suggested to modulate folding, secretion, proteolysis, and interactions.^{12–16} Little is known about phosphorylation of VWF. Solely, the kinase FAM20c has been suggested to phosphorylate VWF at Ser1613 in the A2 domain, thereby modulating ADAMTS13 activity and thrombus formation.¹⁷

Structural Insights into Individual Domains

Atomic-level understanding of VWF is crucial because its hemostatic function arises from precisely orchestrated structural transitions within the massive, multidomain protein. High-resolution structures reveal how individual domains fold, interact, and respond to mechanical forces—insights essential for explaining how VWF captures platelets under shear, anchors to collagen, and regulates its own proteolysis. Structural data also clarify the molecular basis of multimer assembly and storage, processes central to VWF's size-dependent activity. Mapping VWD mutations onto atomic models links genotype to biochemical dysfunction and clinical phenotype. Moreover, structural knowledge enables rational design of therapeutics that modulate VWF–platelet interactions. Thus, atomic-scale insights transform VWF from a biochemical abstraction into a mechanistic framework that connects molecular conformation, force sensing, and pathology. This knowledge is fundamental for advancing both basic and translational hemostasis research. This review thus presents a comprehensive overview of the state-of-the-art structural insights currently available for VWF.

D' and D3 Domains

Shiltagh et al provided the first high-resolution solution structure of the D' region (PDB accession number: 2MHP) in 2014.¹⁸ Using multidimensional NMR spectroscopy and

complementary biophysical analyses, the authors demonstrated that the two subdomains of D', a trypsin inhibitor-like (TIL') domain and a β -sheet-rich E' domain, are stabilized by multiple disulfide bonds that confer structural integrity while preserving localized flexibility. This compact but dynamic architecture enables VWF to maintain a stable yet adaptable binding surface for coagulation factor VIII (FVIII). Residue mapping revealed that FVIII-binding determinants are concentrated on a positively charged surface patch of the TIL' domain, which likely interacts electrostatically with the negatively charged a3 region of the FVIII light chain. This electrostatic complementarity appears central to high-affinity complex formation and stabilization of FVIII in circulation.

The study further correlated structural features with known genetic variants associated with type 2N VWD characterized by defective FVIII binding. Mutations affecting cysteine residues might disrupt multimerization, secretion, and FVIII binding. The three mutations accounting for the majority of reported 2N cases (p.Tyr791Met, p.Arg816Trp, and p.Arg854Gln) are located in immediate proximity to the β 1-to- β 2 loop (marked in [Fig. 2A](#)). Most missense mutations associated with a more severe type 2N phenotype localize near the TIL'/E' interface or within the electrostatic FVIII-binding patch most likely leading to deficiencies in FVIII binding through a perturbation of the β 1-to- β 2 loop.¹⁸

In 2019, Dong et al presented the first high-resolution (2.5 Å) crystal structure of the monomeric D'D3 region of VWF (PDB: 6N29)¹⁹—comprising the D' (TIL'–E') and D3 (VWD3–C8–3–TIL3–E3) modules ([Fig. 2A](#))—thereby adding further understanding about how VWF multimerization and FVIII binding are structurally coupled. In the solved structure, the D3 module forms a large Ca^{2+} -binding VWD3 domain around which the smaller C8–3, TIL3, and E3 subdomains wrap, creating a wedge-shaped architecture with the D' domain projecting outwards ([Fig. 2A](#)). Key cysteine residues that form inter-monomer disulfide bonds during multimerization are buried in the monomeric form at ER-like pH, providing a built-in safeguard against premature

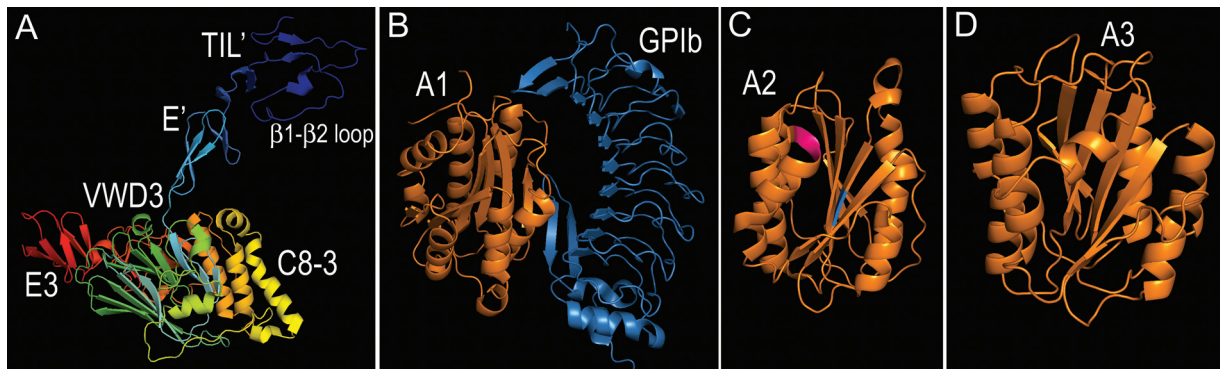


Fig. 2 Structures of domains D' to A3. (A) High-resolution (2.5 Å) crystal structure of the monomeric D'D3 region of VWF (PDB: 6N29).¹⁹ (B) 2.6 Å crystal structure of the extracellular domain of GPIb α (blue) bound to wildtype A1 (orange) (PDB: 1SQ0).²⁴ (C) The 1.9 Å structure of the VWF A2 domain (PDB: 3GXB).²⁵ The vicinal disulfide bond Cys1669–Cys1670 is highlighted in magenta, the Tyr1605–Met1606 ADAMTS13 cleavage site in blue. (D) 1.8 Å crystal structure of the human VWF A3 domain (PDB: 1ATZ).²⁶ All images were generated using PyMOL v2.0 (Schrödinger, LLC).⁴³

multimerization. Release of restrictions due to histidine protonation in the acidic Golgi and Ca²⁺-dependent rearrangement facilitate exposure of these cysteines for head-to-head multimer formation. Critically, the authors show that, in addition to the previously identified TIL' domain of D', the side of the D3 module is also implicated in FVIII binding, thereby extending the binding interface beyond D'. The authors argue that the dual function of D'D3, enabling both multimer assembly and FVIII binding, is mediated by a dynamic structural arrangement that transitions between ER-folded stability and Golgi-activated multimerization.¹⁹

Mapping of known VWF disease-causing mutations onto the structure revealed how perturbation of multimerization and/or FVIII-binding surfaces can result in defective FVIII stabilization and clearance in circulation. The type 2A mutation p.Ser979Asn in C8-3 introduces a putative N-glycosylation site into its interface with VWD3 and is located in close proximity to the Cys1099 essential to multimerization. Thus, p.Ser979Asn may disrupt proper intermodule orientation or structure around Cys1099 required for D3 dimerization. Type 2N mutations mostly are located in D'¹⁸ but some are also found in D3. Mutation p.Asp879Asn in the VWD3 is located near the Ca²⁺-binding site, thereby probably disrupting the dual function of Asp879 in coordinating Ca²⁺ and hydrogen bonding to the backbone of the Ca²⁺-binding loop. Interestingly, p.Asp879Asn causes both type 2A and 2N VWD²⁰ indicating the VWD3 Ca²⁺-binding site to be required for both: efficient D3 dimerization and binding of FVIII.¹⁹

The A Domains

The three A domains of VWF, A1, A2, and A3, form the functional core of the protein's adhesive and regulatory activity in hemostasis. Each domain performs a distinct yet interdependent role: the A1 domain mediates platelet tethering by binding glycoprotein (GP)Ib α on the platelet surface; the A3 domain anchors VWF to exposed subendothelial collagens types I and III at sites of vascular injury, and the A2 domain acts as a mechanical regulator that unfolds under

shear stress to expose the ADAMTS13 cleavage site controlling VWF multimer size and activity. Together, these domains enable VWF to sense hydrodynamic forces, tether platelets to the vessel wall, and prevent uncontrolled thrombosis. Structural elucidation of the A domains has thus been pivotal in defining the molecular mechanisms by which VWF integrates force sensing with receptor recognition to initiate and regulate platelet adhesion under flow.

Since their discovery VWF A-type domains are considered the prototype of a large number of homologous adhesion domains that have later on also been found in a wide range of proteins, including integrins and several collagen types.²¹ The common feature of these domains is the so-called dinucleotide-binding fold consisting of a central β sheet with six strands that is surrounded by seven α helices.²² As described below, indeed all three VWF A domains exhibit this architecture.

Emsley and colleagues reported the first crystal structure of the VWF **A1 domain** (PDB: 1AUQ),²³ defining the atomic basis for its interaction with the platelet receptor GPIb α . The 1.9 Å structure revealed that A1 consists of the characteristic six-stranded β sheet flanked by α helices. Data collected from VWD type 2A and 2B mutations hinted to a putative GPIb α -binding interface at the “upper/front surfaces” of the structure.²³

Dumas et al later on presented the 2.6 Å crystal structure of the extracellular domain of **GPIb α bound to wildtype A1** (PDB: 1SQ0)²⁴ (→Fig. 2B). They showed that A1 remains mostly unchanged in complex with GPIb α compared to the unbound domain. In contrast, GPIb α changes its conformation upon binding with A1. Nonetheless, some conformational divergence was seen in three adjacent regions of A1 upon interaction with GPIb α : the N-terminal end (residues beyond Ser510, inclusively), the C-terminal end (residues beyond Glu700), and the α 1- β 2 loop (residues Arg543–Arg552). In their structure the region around the Cys509–Cys695 bridge linking the A1 termini is well ordered, while residues N-terminal to Asp506 and C-terminal to Pro702 are disordered. In the unliganded A1 structure, these regions

(Asp498-Asp506 and Glu700-Thr705) extend toward the site of GPIIb α interaction. The significance of these extensions is unclear due to water-mediated crystal contacts involving several residues within these termini in the unliganded A1 described by Emsley et al.^{23,24}

The first structure (1.9 Å) of the VWF **A2 domain** (→Fig. 2C) was solved by Zhang et al in 2009 (PDB: 3GXB).²⁵ Among the notable features are an α 4-helix present in A1 which seems to be replaced by a loop and the deeply buried Tyr1605-Met1606 ADAMTS13 cleavage site located within the β 4 strand (→Fig. 2C). Another distinctive feature is the presence of a vicinal disulfide bond (Cys1669-Cys1670) (→Fig. 2C), a motif not observed in other known VWA domains. This disulfide forms an eight-membered ring incorporating both backbone and side-chain atoms, which imparts exceptional local rigidity. Structurally, the C-terminal Ser1671 interacts exclusively with Cys1670, meaning that any tensile force applied to the C terminus is transmitted directly to this disulfide-linked cysteine pair. Because these cysteines constitute the final residues of the α 6-helix and are covalently linked, they share the applied mechanical load. This coupling enables resistance to elongational force through both hydrogen bonds between the Cys1669/Cys1670 amides and the Val1665/Leu1666 carbonyls, as well as through hydrophobic and van der Waals interactions between the Cys side chains and a surrounding hydrophobic pocket formed by Leu1497, Met1528, Ile1535, Leu1603, Tyr1605, and Leu1666. Consequently, the vicinal disulfide serves as a specialized structural element that reinforces the helix terminus, creating a high energy barrier to the initial step of A2 unfolding under force. It effectively acts as a molecular “plug” that stabilizes the hydrophobic core; its disruption initiates the conformational transition leading to A2 domain unfolding.

The mapping of type 2A VWD mutations onto the structure revealed a group of mutations (e.g., p.Arg1597Trp, p.Gly1505Glu, p.Ile1628Thr, p.Glu1638Lys) that lead to destabilization of the fold lowering the force required for unfolding and facilitating premature cleavage in the circulation. Another group (e.g., p.Ser1506Leu, p.Leu1540P) is structurally more disruptive and thus impairs secretion and might affect multimerization.²⁵

Huizinga and colleagues determined the 1.8 Å crystal structure of the human VWF **A3 domain** (PDB: 1ATZ)²⁶ (→Fig. 2D), also revealing the characteristic dinucleotide-binding fold. The structure shows a relatively smooth surface patch enriched in negatively charged residues, interpreted as the collagen-binding interface for collagen types I and III in the vessel wall. Notably, the canonical metal-ion binding motif (DXSXS) present in integrin I domains adopts a loop conformation that is incompatible with ion binding in A3, suggesting that VWF uses charge complementarity rather than metal coordination for collagen recognition. The authors therefore propose that adhesion to collagen is principally driven by electrostatic interactions rather than extensive van der Waals surfaces, consistent with the low affinity of an isolated A3 domain and the requirement for multimeric VWF to achieve stable collagen binding.²⁶

The C Domains

Downstream of the A domains, the VWF monomer contains a series of six tandem C domains (C1–C6) followed by a C-terminal cystine-knot (CK) or CTCK domain. Collectively, the C domains form the so-called “stem” region of VWF and play key roles in conformational extensibility under shear and interaction with platelet integrin α IIb β 3 (also called GPIIb/IIIa). The CK domain mediates mandatory dimerization of VWF monomers in the ER through inter-chain disulfide bonds, thus establishing the basic building block for multimerization and subsequent hemostatic function. Together, the interplay of the C- and CK domains ensures that VWF attains both the elongated multimeric architecture required for shear-activated platelet capture and the stability to resist premature activation.

While there are no structures available for the domains C1, C2, C3, and C5, the group of J. Henning and collaborators presented the first high-resolution solution structures of the VWF C4 and C6 domains. Using NMR spectroscopy, Xu et al resolved that the **C4 domain** (PDB: 6FWN)²⁷ adopts a two-subdomain architecture (SD1 and SD2) connected by a short hinge region around residue Val2547 (→Fig. 3A). The structure reveals five intra- and inter-subdomain disulfide bonds (one of which is unique to C4) and demonstrates that slow conformational motions around the hinge permit positional variation between the subdomains. The study further shows that a clinically observed prothrombotic gain-of-function variant (p.Phe2561Tyr) does not enhance integrin binding per se but likely alters the relative orientation of the subdomains and/or neighboring domains, thereby lowering the threshold for VWF-platelet rolling aggregate formation. These structural dynamics of C4 thereby provide a mechanistic foundation for how the C domain stem may switch between compact and extended states, and how subtle mutation-induced alterations can shift VWF from a latent to a hyperadhesive state.²⁷

Chen and co-workers elucidated the structure and dynamic behavior of the wildtype **C6 domain** (PDB: 7P4N)²⁸ and determined that the fold of C6 is highly similar to the C4 domain with flexibility between its two subdomains SD1 and SD2 (→Fig. 3B). Both C4 and C6 share the same disulfide pattern different from the other three determined C domain structures of collagen 2A, CV-2, or CCN3. Solving the structures of the remaining VWF C domains will answer the question whether C domains with four disulfide bonds, as in C4 and C6, or with five disulfide bonds, as present in the C domains of collagen 2A, CV-2, or CCN3, are more common in VWF. Differences between the C4 and C6 domains are the increased slow conformational exchange of C6 within SD1²⁸ and the absence of the RGD binding motif in C6, altering the relative position of the SD1 β -sheets to each other compared to C4.²⁸

CK Domain

Zhou and Springer solved the crystal structure of the C-terminal cystine-knot (CK/CTCK) domain of VWF (PDB: 4NT5),⁸ providing key insights into the VWF dimerization process. The CK domain monomer is elongated and features

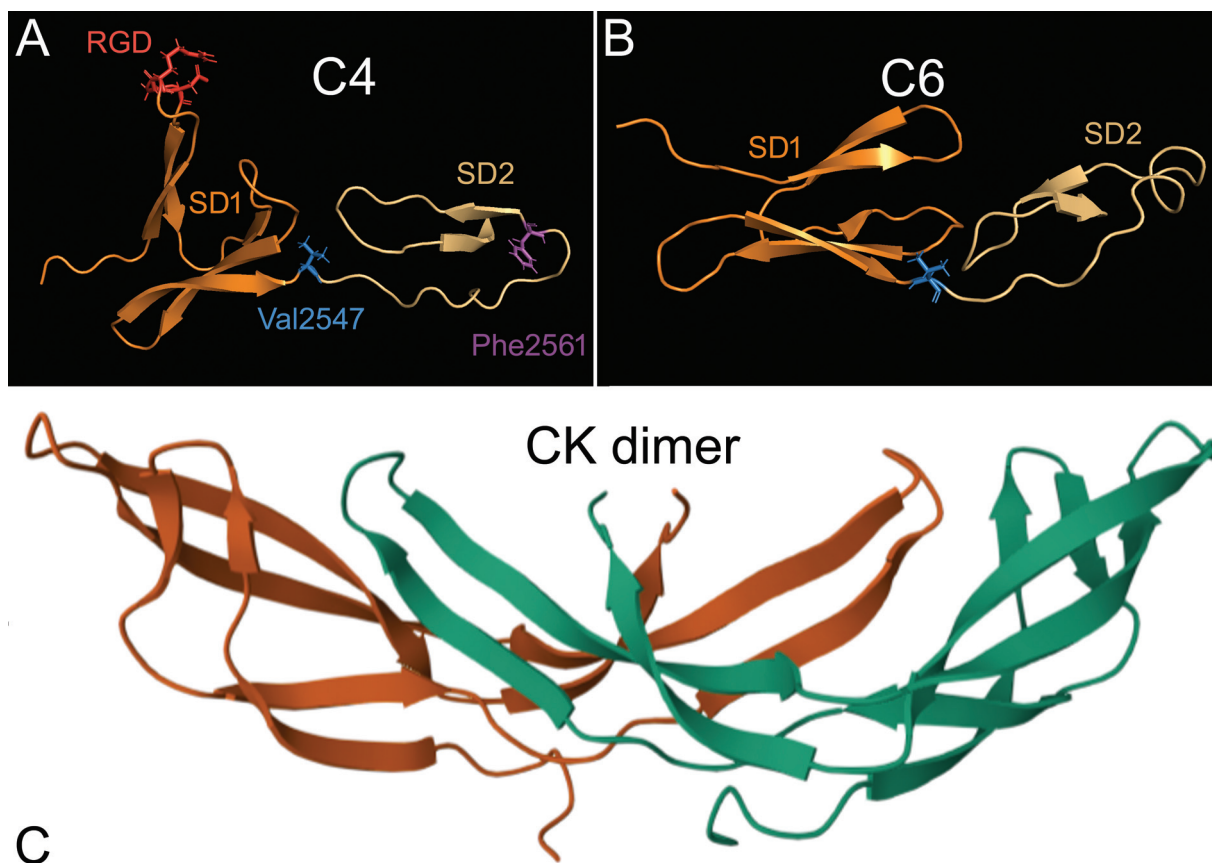


Fig. 3 Structures of C4, C6, and the CDCK dimer. (A) NMR structure of VWF C4 (PDB: 6FWN).²⁷ Subdomains SD1 and SD2 are shown in dark and light orange, respectively. The GPIIb/IIIa binding RGD motif is highlighted in red, the hinge Val2547 in blue, and Phe2561, often mutated to Tyr in a common polymorphism, in magenta. (B) NMR structure of VWF C6 (PDB: 7P4N).²⁸ Subdomains SD1 and SD2 are shown in dark and light orange, respectively. (C) Crystal structure of the C-terminal cystine-knot (CK/CTCK) domain of VWF arranged in an antiparallel dimer (PDB: 4NT5).⁶ One CK monomer is shown in orange, the second in green. All images generated using PyMOL v2.0 (Schrödinger, LLC).⁴³

two β -ribbons and four intra-chain disulfide bonds (three of which reside within the canonical knot). Antiparallel dimerization occurs via formation of a super β -sheet, burial of approximately 1,500 Å² of surface area (approximately 32% of each monomer's surface) and three inter-chain disulfides (→Fig. 3C), yielding a robust interface able to resist hydrodynamic force and disulfide reduction. The structure explains how VWF achieves tail-to-tail dimerization in the ER, which is a prerequisite for subsequent head-to-head multimer formation in the Golgi. The authors emphasize that perturbation of cysteine residues Cys2771 and Cys2773, involved in inter-chain disulfides, leads to VWD type 2 while intra-chain disulfide-deleting mutation results in VWD type 3.⁸

Multimerization and Storage

In 2022, two studies addressed the long-standing question in the biosynthesis of VWF about how the N-terminal propeptide (D1D2) drives head-to-head multimerization and packaging into helical tubules in WPBs. Zeng et al presented high-resolution cryo-electron-microscopy (cryo-EM) reconstructions of VWF N-terminal fragments D1D2D'D3 assembled into WPB-like tubules, reaching resolutions of approximately 2.85 Å (PDB

7WPP for 1 repeating unit, PDB 7WPQ for 2 repeating units, and PDB 7WQT for 8 repeating units; →Fig. 4).²⁹

Key mechanistic insights that emerge from this study are that the D2 domains of two pro-VWF molecules form a homodimer interface (D2:D2) at acidic pH mimicking the trans-Golgi/immature WPB environment. This propeptide homodimer then recruits two D'D3 domains, yielding an intertwined D1D2–D'D3 complex. Successive stacking of these basic units, mediated by intermolecular D1:D2 interactions, arranges the complexes into a right-handed helical tubule. In this arrangement, the two D'D3 modules are juxtaposed face-to-face, thereby spatially promoting the critical inter-chain disulfide bonds that link adjacent dimers into ultra-large VWF multimers.²⁹

These insights are extended by Anderson et al showing that the A1 domain is an integral component of the tubule wall, as the A1 domain cross-links successive helical turns of the tubule, thus promoting longer tubule formation (PDB: 8D3C).³⁰

In summary, these studies offer a detailed mechanistic view of how VWF self-assembles into concatemers: tubule formation driven by acidic charge neutralization, elongation aided by the A1 domain, and internal rearrangement of cysteines via a disulfide-exchange pathway to yield stable, linked multimers.

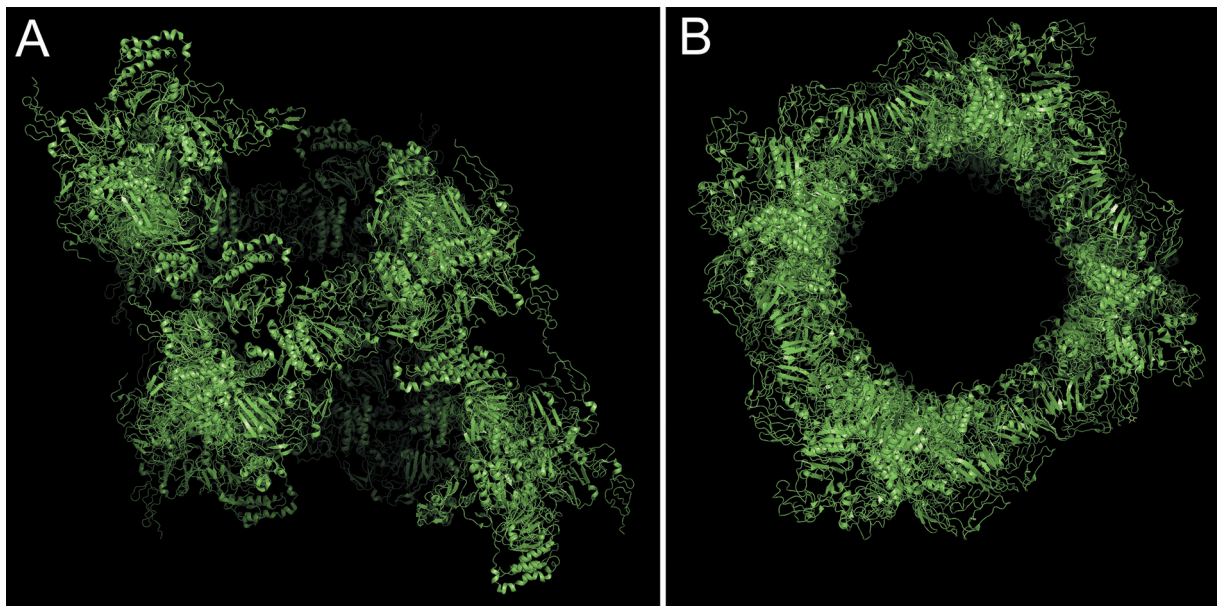


Fig. 4 Structure of D1D2D'D3 tubules. High-resolution cryo-electron-microscopy reconstructions of VWF N-terminal fragments D1D2D'D3 assembled into WPB-like tubules, reaching resolutions of approximately 2.85 Å (PDB: 7WQT for 8 repeating units) shown from the side (A) and the top (B).²⁹ All images generated using PyMOL v2.0 (Schrödinger, LLC).⁴³

Therapeutic Implications of Structural Insights

The growing body of high-resolution structural data on the VWF A1 domain has not only deepened our understanding of its role in platelet adhesion but also provided a framework for the rational design of targeted therapeutics. Since the A1 domain is the central mechanosensitive module that mediates VWF binding to GPIIb α it has been the main focus for the development of therapeutic agents. Structural elucidation of A1 in complex with various ligands, including antibodies, toxins, aptamers, and nanobodies,^{31–34} has revealed distinct mechanisms by which its activity can be modulated. These studies have shown that A1 can adopt conformations ranging from low- to high-affinity states for GPIIb α , and that therapeutic molecules can exploit this conformational flexibility to inhibit, stabilize, or reorient the domain. By resolving these complexes at atomic resolution, key epitopes, interaction surfaces, and conformational changes have been identified explaining both natural regulatory mechanisms and drug actions.

This section exemplarily summarizes two landmark structural studies that have shaped our current molecular understanding of A1-targeted therapeutics. The described structures illustrate examples of strategies by which the VWF–platelet interaction can be disrupted or modulated. Together, they highlight how structural biology continues to guide the development of next-generation therapies for VWD as well as TTP.

A1-binding DNA Aptamer ARC1172

The high-resolution structure of VWF A1 bound to the DNA aptamer ARC1172 (PDB: 3HXO) was solved by Huang et al in

2009.³³ In the crystal structure of a VWF A1–ARC1172 complex (–Fig. 5A), the aptamer forms a three-stem structure of mainly B-form DNA with three noncanonical base pairs and nine unpaired residues, six of which are stabilized by base–base or base–deoxyribose stacking interactions. The aptamer–A1 interface involves interactions between Arg, Lys, and Gln residues stabilized by hydrogen bonds with adjacent bases. ARC1172 binding hinders interaction with GPIIb α explaining the antithrombotic activity of ARC1172 observed during *in vitro* platelet adhesion assays and *in vivo* in a cynomolgus monkey carotid electrical injury thrombosis model.³⁵ The structural data explain how ARC1172 sterically and electrostatically prevents the A1 domain from binding GPIIb α , thereby reducing platelet adhesion under shear and laid the ground for the development of further antithrombotic aptamers, such as ARC1779, which was shown to increase VWF levels and platelet counts in patients with type 2B VWD.³⁶

The VWF A1 Domain in Complex with Caplacizumab

The crystal structure (1.60 Å resolution) of the VWF A1 domain in complex with the therapeutic nanobody caplacizumab (PDB: 7EOW) was solved by Lee et al.³⁴ This bivalent single-domain antibody is the first FDA-approved anti-VWF therapy against acquired TTP. The structural analysis reveals that caplacizumab binds to the “bottom” face of the A1 domain (–Fig. 5B), i.e., on the side opposite to the canonical GPIIb α binding surface. Remarkably, the binding does not sterically occlude the GPIIb α interface, suggesting an indirect mechanism of inhibition. Instead, the authors show that nanobody binding stabilizes a particular conformation of the N-terminus and a loop (α 1 β 2 loop) of A1 that is

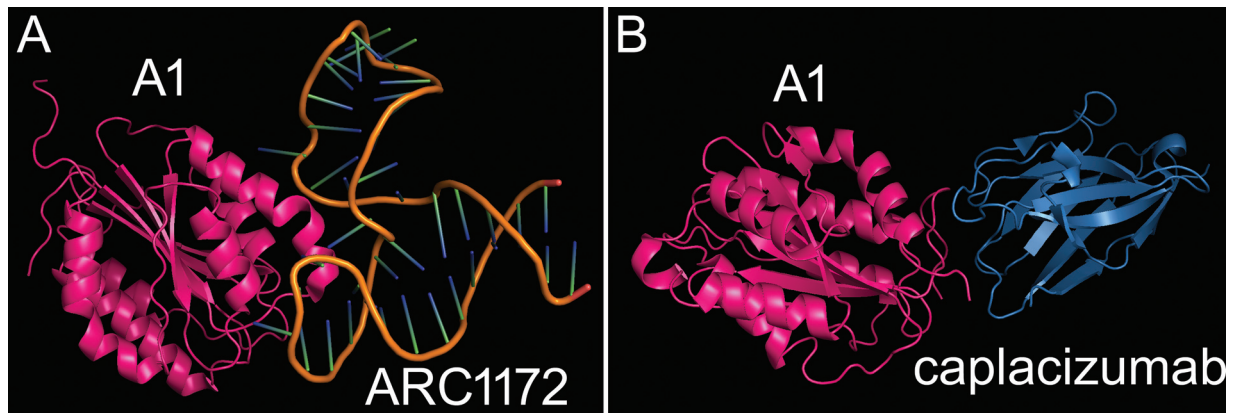


Fig. 5 The VWF A1 domain in complex with therapeutic agents. (A) Crystal structure of VWF A1 (magenta) bound to the DNA aptamer ARC1172 (blue and orange) (PDB: 3HXO).³³ (B) Crystal structure (1.60 Å resolution) of the VWF A1 domain (magenta) in complex with the therapeutic nanobody caplacizumab (blue) (PDB: 7EOW).³⁴ All images generated using PyMOL v2.0 (Schrödinger, LLC).⁴³

incompatible with high-affinity GPIIb α binding. Thus, caplacizumab functions by “arresting” the A1 domain in a suboptimal conformation for platelet binding rather than by direct competition.³⁴

Structural Changes in VWF upon Exposure to Shear Stress

Cryo-EM and atomic force microscopy (AFM) imaging were used to gain structural insights into the VWF stem region.^{6,37} As these methods are limited to static conditions, even when “pre-stretching” approaches are applied prior to imaging,³⁸ different methods need to be used to gather detailed information about the dynamic stem-opening and closing of VWF. Löff et al presented a modular magnetic-tweezers (MT)-based method for multiplexed single-molecule force spectroscopy, capable of probing protein unfolding/refolding dynamics at very low forces (<1 pN). This approach expands on prior techniques (such as AFM or optical tweezers) by improving throughput, force stability, and access to physiologically relevant low-force regimes. The method hinges on elastin-like polypeptide (ELP) linkers and short peptide tags for specific protein attachment, allowing minimal interference with the protein of interest and enabling high yields of single-molecule tethers. The measurements reveal two key findings for VWF: first, the A2 domain’s unfolding/refolding kinetics and A2 stabilization by Ca²⁺; and second, a reversible transition in the C-terminal stem region of VWF at forces around 1 pN. These low-force conformational changes likely represent mechanical steps (“unzipping” of the C domain stem) in VWF mechano-activation when exposed to shear in the vasculature. Quantitatively, at forces of about 1 pN, reversible transitions with a maximum contour length increase of approximately 50 nm were observed. Increasing force (0.5–1.5 pN) led to a systematic shift in the population toward higher tether extensions, which were interpreted as less compact “unzipped” conformations of the VWF stem. The overall force response of the VWF stem exhibits a multistate behavior with different levels of stem zipping which is consistent with AFM imaging showing populations

of dimers with fully closed, partially open, and fully open stems with different numbers of C domains interacting.³⁹

Future Perspectives and Challenges in Structural Analysis of VWF

Despite the impressive progress in resolving atomic structures of individual VWF domains and assemblies, major challenges remain in achieving a truly integrated structural understanding of this extraordinarily large and dynamic protein (summarized in [Table 1](#)). Besides solving the structures of the remaining C domains C1, C2, C3, and C5, one of the foremost goals is to elucidate the architecture of VWF dimers and multimers in their native, full-length context. Although cryo-EM and X-ray crystallography have provided insights into isolated domains or limited domain assemblies, the structure of VWF full-length dimers or multimers as well as the quaternary organization of ultra-large multimers within tubular storage forms in WPBs are not yet fully defined. Capturing these supramolecular assemblies at high resolution remains technically challenging due to their size, flexibility, and heterogeneity. Innovative methods, such as Cryo-ET of WPBs with subsequent subtomogram averaging and correlative light and electron microscopy (CLEM), could offer novel pathways to gain deeper insights into WPB organization.

Another frontier lies in understanding the dynamic behavior of VWF under shear stress. Current single-molecule studies using AFM,⁴⁰ optical tweezers,⁴¹ and dual color TIRF imaging coupled with microfluidic flow assays⁴² have revealed force-induced unfolding of the A2 domain and conformational activation of A1, but structural visualization of these transitions at atomic or near-atomic resolution remains elusive. Integrative approaches that might combine cryo-electron tomography, time-resolved cryo-EM, and molecular dynamics simulations could illuminate how VWF multimers extend, uncoil, and expose adhesive sites in response to mechanical forces. Such dynamic structural mapping would bridge the gap between static crystallographic models and the protein’s real behavior in circulation.

Table 1 Concise tabular summary of the open research questions

Open research question	Relevance	Possible methodological approaches
Structures of C domains C1, C2, C3, and C5	Necessary for completing the domain-level structural map of VWF	<ul style="list-style-type: none"> ➤ X-ray crystallography ➤ Cryo-EM ➤ NMR
What is the architecture of full-length VWF dimers and multimers in their native state at different pH values?	Critical for understanding how VWF assembles into hemostatically active multimers and disease mechanisms in VWD; structure/phenotype relationship	<ul style="list-style-type: none"> ➤ Cryo-EM single-particle analysis ➤ Cryo-electron tomography (cryo-ET) ➤ Integrative modeling ➤ Cross-linking mass spectrometry
How are ultra-large multimers organized within Weibel–Palade body (WPB) tubules? (at high resolution)	Essential for explaining how VWF is tubulated, stored, and released	<ul style="list-style-type: none"> ➤ Cryo-ET of WPBs with subsequent subtomogram averaging ➤ Correlative light and electron microscopy (CLEM)
How do VWF multimers structurally reorganize under shear stress?	Mechanical activation and deactivation are central to VWF function in circulation; needed to link force-dependent behavior to molecular structure, function, and disease mechanisms	<ul style="list-style-type: none"> ➤ Time-resolved cryo-EM ➤ Cryo-ET under flow ➤ Molecular dynamics (MD) simulations ➤ Microfluidics-coupled imaging ➤ Magnetic tweezers
What are the structural intermediates during A1 activation and A2 unfolding under force?	Explains how binding and cleavage sites are exposed; crucial for understanding thrombosis, TTP, and shear-induced activation	<ul style="list-style-type: none"> ➤ Atomic force spectroscopy ➤ Magnetic tweezers ➤ MD simulations
How do VWF multimers extend, uncoil, and expose binding sites in real time?	Bridging the gap between static structures and dynamic physiological function; informs multiscale mechanobiology	<ul style="list-style-type: none"> ➤ Integrative hybrid methods combining cryo-ET, time-resolved cryo-EM, MD, TIRF, and high-speed fluorescence imaging
How can therapeutics selectively modulate pathological vs. physiological VWF activity?	Preventing thrombosis without impairing hemostasis is a major clinical need	<ul style="list-style-type: none"> ➤ Structure-based drug design ➤ Engineering allosteric modulators ➤ Mapping drug-resistant variants ➤ Ligand-stabilized state modeling
Can small molecules be designed to stabilize specific VWF conformational states?	Would produce (orally bioavailable) agents with tunable potency; expands beyond biologics (nanobodies, aptamers)	<ul style="list-style-type: none"> ➤ Computational screening ➤ Fragment-based design ➤ AI-driven docking ➤ MD-guided conformational targeting
How can static structural data be integrated with force-dependent and cellular-scale dynamics?	Achieving a unified model of VWF from storage to activation to clearance requires multiscale understanding	<ul style="list-style-type: none"> ➤ Multiscale modeling ➤ Integrative structural biology ➤ Live-cell imaging ➤ Correlative cryo-microscopy ➤ Machine learning–based integration

Note: Open questions, their relevance, and possible methodological approaches.

From a translational perspective, structural studies are increasingly shaping therapeutic innovation. The success of the nanobody caplacizumab and the development of anti-VWF aptamers underscore the potential of structure-guided drug design. However, a major challenge is to design agents that selectively modulate pathological VWF activity without compromising physiological hemostasis. Future efforts will likely focus on computational screening of small molecules that stabilize specific conformational states of VWF and structure-based engineering of allosteric—possibly orally bioavailable—modulators to gain the ability to fine-tune VWF activity. These could, for example, be used to partially reduce shear-induced activation to achieve normalization of hyperactive VWF variants.

Ultimately, the next phase of VWF structural biology will depend on multiscale integration, combining high-resolu-

tion static structures with dynamic, force-dependent, and cellular-scale imaging, to achieve a cohesive molecular and mechanistic understanding of how VWF transitions between storage, activation, and clearance.

Conclusion

Structural analysis of VWF has revealed a protein finely tuned for vascular hemostasis through modular design and mechanosensitivity. Each domain contributes specialized functions, while inter-domain interactions regulate activation and proteolysis. Diseases such as VWD and TTP exemplify how structural perturbations disrupt this balance. The fusion of structural biology with clinical hemastaseology promises not only deeper mechanistic insight but also innovative therapies.

Conflict of Interest

The authors declare that they have no conflict of interest.

References

- Sadler JE. Biochemistry and genetics of von Willebrand factor. *Annu Rev Biochem* 1998;67:395–424
- Mansouri Taleghani M, von Krogh AS, Fujimura Y, et al. Hereditary thrombotic thrombocytopenic purpura and the hereditary TTP registry. *Hamostaseologie* 2013;33(02):138–143
- Furlan M, Robles R, Solenthaler M, Wassmer M, Sandoz P, Lämmle B. Deficient activity of von Willebrand factor-cleaving protease in chronic relapsing thrombotic thrombocytopenic purpura. *Blood* 1997;89(09):3097–3103
- Gerritsen HE, Robles R, Lämmle B, Furlan M. Partial amino acid sequence of purified von Willebrand factor-cleaving protease. *Blood* 2001;98(06):1654–1661
- Crawley JT, de Groot R, Xiang Y, Luken BM, Lane DA. Unraveling the scissile bond: how ADAMTS13 recognizes and cleaves von Willebrand factor. *Blood* 2011;118(12):3212–3221
- Zhou YF, Eng ET, Zhu J, Lu C, Walz T, Springer TA. Sequence and structure relationships within von Willebrand factor. *Blood* 2012;120(02):449–458
- Lippok S, Kolšek K, Löf A, et al. von Willebrand factor is dimerized by protein disulfide isomerase. *Blood* 2016;127(09):1183–1191
- Zhou YF, Springer TA. Highly reinforced structure of a C-terminal dimerization domain in von Willebrand factor. *Blood* 2014;123(12):1785–1793
- Stockschlaeder M, Schneppenheim R, Budde U. Update on von Willebrand factor multimers: focus on high-molecular-weight multimers and their role in hemostasis. *Blood Coagul Fibrinolysis* 2014;25(03):206–216
- Nightingale T, Cutler D. The secretion of von Willebrand factor from endothelial cells; an increasingly complicated story. *J Thromb Haemost* 2013;11(Suppl 1):192–201
- Giblin JP, Hewlett LJ, Hannah MJ. Basal secretion of von Willebrand factor from human endothelial cells. *Blood* 2008;112(04):957–964
- McKinnon TA, Goode EC, Birdsey GM, et al. Specific N-linked glycosylation sites modulate synthesis and secretion of von Willebrand factor. *Blood* 2010;116(04):640–648
- McGrath RT, van den Biggelaar M, Byrne B, et al. Altered glycosylation of platelet-derived von Willebrand factor confers resistance to ADAMTS13 proteolysis. *Blood* 2013;122(25):4107–4110
- Nowak AA, Canis K, Riddell A, Laffan MA, McKinnon TA. O-linked glycosylation of von Willebrand factor modulates the interaction with platelet receptor glycoprotein Ib under static and shear stress conditions. *Blood* 2012;120(01):214–222
- Solecka BA, Weise C, Laffan MA, Kannicht C. Site-specific analysis of von Willebrand factor O-glycosylation. *J Thromb Haemost* 2016;14(04):733–746
- Wagner DD, Mayadas T, Marder VJ. Initial glycosylation and acidic pH in the Golgi apparatus are required for multimerization of von Willebrand factor. *J Cell Biol* 1986;102(04):1320–1324
- Da Q, Nolasco J, Khatlani T, Maria F, Cruz MA, Vijayan KV. FAM20c-mediated serine 1613 phosphorylation in the A2 domain of von Willebrand factor regulates ADAMTS13 activity and thrombus formation. *Blood* 2015;126(23):236–236
- Shiltagh N, Kirkpatrick J, Cabrita LD, et al. Solution structure of the major factor VIII binding region on von Willebrand factor. *Blood* 2014;123(26):4143–4151
- Dong X, Leksa NC, Chhabra ES, et al. The von Willebrand factor D'D3 assembly and structural principles for factor VIII binding and concatemer biogenesis. *Blood* 2019;133(14):1523–1533
- Jorieux S, Gaucher C, Goudemand J, Mazurier C. A novel mutation in the D3 domain of von Willebrand factor markedly decreases its ability to bind factor VIII and affects its multimerization. *Blood* 1998;92(12):4663–4670
- Colombatti A, Bonaldo P. The superfamily of proteins with von Willebrand factor type A-like domains: one theme common to components of extracellular matrix, hemostasis, cellular adhesion, and defense mechanisms. *Blood* 1991;77(11):2305–2315
- Romijn RA, Bouma B, Wuyster W, et al. Identification of the collagen-binding site of the von Willebrand factor A3-domain. *J Biol Chem* 2001;276(13):9985–9991
- Emsley J, Cruz M, Handin R, Liddington R. Crystal structure of the von Willebrand factor A1 domain and implications for the binding of platelet glycoprotein Ib. *J Biol Chem* 1998;273(17):10396–10401
- Dumas JJ, Kumar R, McDonagh T, et al. Crystal structure of the wild-type von Willebrand factor A1-glycoprotein Ibalpha complex reveals conformation differences with a complex bearing von Willebrand disease mutations. *J Biol Chem* 2004;279(22):23327–23334
- Zhang Q, Zhou YF, Zhang CZ, Zhang X, Lu C, Springer TA. Structural specializations of A2, a force-sensing domain in the ultralarge vascular protein von Willebrand factor. *Proc Natl Acad Sci U S A* 2009;106(23):9226–9231
- Huizinga EG, Martijn van der Plas R, Kroon J, Sixma JJ, Gros P. Crystal structure of the A3 domain of human von Willebrand factor: implications for collagen binding. *Structure* 1997;5(09):1147–1156
- Xu ER, von Bülow S, Chen PC, et al. Structure and dynamics of the platelet integrin-binding C4 domain of von Willebrand factor. *Blood* 2019;133(04):366–376
- Chen PC, Kutzki F, Mojzisch A, et al. Structure and dynamics of the von Willebrand Factor C6 domain. *J Struct Biol* 2022;214(04):107923
- Zeng J, Shu Z, Liang Q, et al. Structural basis of von Willebrand factor multimerization and tubular storage. *Blood* 2022;139(22):3314–3324
- Anderson JR, Li J, Springer TA, Brown A. Structures of VWF tubules before and after concatemerization reveal a mechanism of disulfide bond exchange. *Blood* 2022;140(12):1419–1430
- Celikel R, Varughese KI, Madhusudan, Yoshioka A, Ware J, Ruggeri ZM. Crystal structure of the von Willebrand factor A1 domain in complex with the function blocking NMC-4 Fab. *Nat Struct Biol* 1998;5(03):189–194
- Fukuda K, Doggett TA, Bankston LA, Cruz MA, Diacovo TG, Liddington RC. Structural basis of von Willebrand factor activation by the snake toxin botrocetin. *Structure* 2002;10(07):943–950
- Huang RH, Fremont DH, Diener JL, Schaub RG, Sadler JE. A structural explanation for the antithrombotic activity of ARC1172, a DNA aptamer that binds von Willebrand factor domain A1. *Structure* 2009;17(11):1476–1484
- Lee HT, Park UB, Jeong TJ, et al. High-resolution structure of the vWF A1 domain in complex with caplacizumab, the first nanobody-based medicine for treating acquired TTP. *Biochem Biophys Res Commun* 2021;567:49–55
- Diener JL, Daniel Lagassé HA, Duerschmied D, et al. Inhibition of von Willebrand factor-mediated platelet activation and thrombosis by the anti-von Willebrand factor A1-domain aptamer ARC1779. *J Thromb Haemost* 2009;7(07):1155–1162
- Jilma-Stohlawetz P, Knöbl P, Gilbert JC, Jilma B. The anti-von Willebrand factor aptamer ARC1779 increases von Willebrand factor levels and platelet counts in patients with type 2B von Willebrand disease. *Thromb Haemost* 2012;108(02):284–290
- Löf A, König G, Schneppenheim S, et al. Advancing multimer analysis of von Willebrand factor by single-molecule AFM imaging. *PLoS One* 2019;14(01):e0210963
- Csányi MC, Salamon P, Feller T, Bozót T, Hársfalvi J, Kellermayer MSZ. Structural hierarchy of mechanical extensibility in human

- von Willebrand factor multimers. *Protein Sci* 2023;32(01): e4535
- 39 Löff A, Walker PU, Sedlak SM, et al. Multiplexed protein force spectroscopy reveals equilibrium protein folding dynamics and the low-force response of von Willebrand factor. *Proc Natl Acad Sci U S A* 2019;116(38):18798–18807
- 40 Müller JP, Löff A, Mielke S, et al. pH-dependent interactions in dimers govern the mechanics and structure of von Willebrand factor. *Biophys J* 2016;111(02):312–322
- 41 Arya M, Anvari B, Romo GM, et al. Ultralarge multimers of von Willebrand factor form spontaneous high-strength bonds with the platelet glycoprotein Ib-IX complex: studies using optical tweezers. *Blood* 2002;99(11):3971–3977
- 42 Fu H, Jiang Y, Yang D, Scheiflinger F, Wong WP, Springer TA. Flow-induced elongation of von Willebrand factor precedes tension-dependent activation. *Nat Commun* 2017;8(01):324
- 43 Schrödinger, LCC, The PyMOL Molecular Graphics System. Version 1.5.0.4 2010